Chemical Nonequilibrium Boundary Layer

F G BLOTTNER*
General Electric Company, King of Prussia, Pa

The nonequilibrium boundary layer is considered as a binary mixture of atoms and molecules with finite dates of dissociation and recombination To obtain accurate solutions to the partial differential equations for this type of flow without any necessary simplifying assumptions, an implicit finite-difference scheme is developed for solving these equations with a digital computer Accurate solutions to the nonequilibrium boundary-layer equations have been obtained in a reasonable amount of computer time and are presented for a flat plate, cone, and hemisphere cylinder The results show that the nonequilibrium boundary-layer temperature and composition can be considerably different from local equilibrium and frozen results For a cone at 21,000 fps and 100,000 ft alt, the computations show that, at 60 ft from the tip, the flow has not reached equilibrium

Nomenclature

$A_n, B_n, C_n D_n$ = coefficient matrices in the difference equation (A4)
c_i = mass fraction of species i, ρ_i/ρ
c_f = local skin friction coefficient, $2\tau_b/(\rho_r u_e^2)$
c_{pi} = specific heat at constant pressure of species i, ft²/sec² °R
$\bar{c}_p$ = specific heat at constant pressure of the mixture $\Sigma_i c_i c_{pi}$, ft²/sec² °R
$\mathfrak{D}_{ij}$ = binary diffusion coefficients, ft²/sec
D_i^T = thermal diffusion coefficient, lb sec/ft
f' = velocity ratio, u/u_e
h = enthalpy, $\Sigma_i c_i h_i$, ft²/sec²
h_i = enthalpy of species i, ft²/sec²
k = thermal conductivity of mixture, lb/sec °R
l = density-viscosity product, $\rho\mu/(\rho\mu)_r$
Le = Lewis-Semenov number, $\bar{c}_p \rho \mathfrak{D}_{ij}/k$
Le^T = thermal Lewis-Semenov number, $\bar{c}_p D_i^T/k$
$\bar{M}$ = molecular weight of the mixture, $1/(\Sigma_i c_i/M_i)$, lb/lb-mole
M_i = molecular weight of species i, lb/lb mole
Nu = Nusselt number
Pr = Prandtl number, $\bar{c}_p \mu/k$
p = pressure, psf
R = universal gas constant, lb ft²/(lb-mole sec² °R)
Re_x = Reynolds number based on distance along body and reference conditions, $\rho_r u\, x/\mu_r$
r = distance from axis in axisymmetric problems, ft
T = temperature, °R
u, v = velocity components tangential and normal to body surface, fps
V = transformed normal velocity
$\dot{w}_i$ = mass rate of formation of species i, lb sec²/ft⁴ sec
w_n = vector for dependent variables
x = distance along surface from leading edge or stagnation point, ft
y = distance along normal from surface, ft
β = pressure gradient parameter
δ^* = displacement thickness, ft
η = transformed y coordinate
ξ = transformed x coordinate, lb² sec²/ft^{2(2−j)}
$\Delta\eta, \Delta\xi$ = step sizes in transformed coordinates
θ = temperature ratio, T/T_e
μ = viscosity, lb sec/ft²
ρ = density, lb sec²/ft⁴
ρ_i = density of species i, lb sec²/ft⁴
τ = shear stress psf

Subscripts

A = atom
b = conditions at body surface
e = conditions at outer edge of boundary layer
m = designation of mesh point in ξ direction, $\xi = (m-1)\Delta\xi$
n = designation of mesh point in η direction, $\eta = (n-1)\Delta\eta$
M = molecule
r = quantities evaluated at some reference condition
s = conditions at stagnation point or leading edge
∞ = freestream conditions

Presented as Preprint 63 443 at the AIAA Conference on Physics of Entry into Planetary Atmospheres, Cambridge, Mass , August 26–28, 1963; revision received November 26, 1963 Based upon work sponsored by the Ballistic Missiles Division of the U S Air Force under Contract AF 04(694)-222 The author wishes to acknowledge E Meyer of C-E-I R, Inc for programming the finite difference scheme and obtaining the numerical solution The author also acknowledges C Boyer and C Todd of General Electric for programming and obtaining the other numerical results presented

* Research Engineer Gas Dynamics, Space Sciences Laboratory Member AIAA

I Introduction

FOR a complete investigation of the boundary layer on bodies at hypersonic velocities, it is necessary to consider chemical reactions in the flow With finite chemical reaction rates that allow nonequilibrium flow, the boundary-layer equations can only be reduced to ordinary differential equations at the stagnation point of a blunt body The stagnation problem with a binary mixture has been considered by Fay and Riddell,[1] whereas air with several species has been investigated by Moore and Pallone [2] The flow away from the stagnation point and along bodies has been considered only with approximate procedures Chung and Anderson[3,4] have used an integral method to obtain the boundary-layer flow on an adiabatic and noncatalytic flat plate and around a noncatalytic sphere-cone with specified wall temperature In the first example, the fluid was taken as oxygen atoms and molecules whereas for the latter case, oxygen atoms and nitrogen atoms and molecules are employed for the gas model Rae[5] has obtained the nonequilibrium boundary layer of a diatomic gas near the leading edge of a flat plate by employing a double expansion in terms of the distance along the surface and the atom mass fraction Additional assumptions have been used, such as Prandtl and Lewis number equal to one, in the foregoing papers

The ideal of local similarity has been employed by Levinsky and Brainerd[6] to obtain the nonequilibrium boundary layer for a five species air model along a nozzle This procedure can give reasonable results for equilibrium and frozen boundary layers, as shown by Lees,[7] Kemp, Rose, and Detra,[8] and Moore [9] No complete investigation of the validity of local similarity for nonequilibrium boundary layers has been per-

formed; however, reasonable results are obtained for a flat-plate flow as shown by Blottner [10] Even if similar solutions are sufficiently precise, they are difficult to obtain, since accurate initial estimates are required for the boundary conditions that are being iterated Hence, a large amount of time and effort is required to acquire the solution with this procedure

For the present analysis, the gas in the nonequilibrium boundary layer is taken as a binary mixture of atoms and molecules with finite rates of dissociation and recombination To obtain accurate solutions of these partial differential equations without any necessary simplifying assumptions, an implicit finite-difference scheme is developed for solving these equations This method is similar to the procedure investigated by Flügge-Lotz and Blottner [11] The important difference between the present approach and that of Ref 11 is the manner in which the boundary-layer equations are trans formed before the finite difference approximation is made The coordinate normal to the wall is stretched in such a way that the boundary layer is of nearly uniform thickness in the transformed plane This procedure allows solution of the boundary-layer equations from the stagnation point or from a leading edge with similar solutions as initial profiles Also, this method permits larger steps to be taken along the body, since the profiles do not change rapidly in the transformed coordinates

The boundary conditions at the outer edge of the boundary layer are obtained from the inviscid flow along the body With the pressure distribution assumed known along the body, a set of ordinary differential equations which govern this flow, are solved to obtain the velocity, temperature, and atom mass fraction at the edge of the boundary layer The following boundary conditions at the wall are considered: zero normal and tangential velocities, specified wall tempera ture or zero heat transfer, and catalytic or noncatalytic wall

The boundary-layer flow on an insulated and noncatalytic flat plate has been obtained and is compared with the results of Chung and Anderson[3] and Rae [5] The boundary layer on a flat plate with specified wall temperature and catalytic wall has also been considered Calculations for a hemisphere-cylinder and a cone at various altitudes are presented

II Method of Analysis

A System of Equations

The boundary-layer equations for a chemically reacting binary mixture of atoms and molecules are as follows:

Continuity

$$\frac{\partial}{\partial x}(\rho u r_b{}^j) + \frac{\partial}{\partial y}(\rho v r_b{}^j) = 0 \tag{1a}$$

Momentum

$$\rho u \frac{\partial u}{\partial x} + \rho v \frac{\partial u}{\partial y} = -\frac{dp_e}{dx} + \frac{\partial}{\partial y}\left(\mu \frac{\partial u}{\partial y}\right) \tag{1b}$$

Energy

$$\bar{c}_p \rho u \frac{\partial T}{\partial x} + \bar{c}_p \rho v \frac{\partial T}{\partial y} = u \frac{dp}{dx} + \mu \left(\frac{\partial u}{\partial y}\right)^2 + \frac{\partial}{\partial y}\left(k \frac{\partial T}{\partial y}\right) - \Sigma_i \dot{w}_i h_i + \Sigma_i \left[c_{pi} \left(\rho \mathfrak{D}_{ij} \frac{\partial c_i}{\partial y} + \frac{D_i{}^T}{T} \frac{\partial T}{\partial y} \right) \right] \frac{\partial T}{\partial y} \tag{1c}$$

Conservation of Species

$$\rho u \frac{\partial c_i}{\partial x} + \rho v \frac{\partial c_i}{\partial y} = \frac{\partial}{\partial y}\left(\rho \mathfrak{D}_{ij} \frac{\partial c_i}{\partial y} + \frac{D_i{}^T}{T} \frac{\partial T}{\partial y}\right) + \dot{w}_i \tag{1d}$$

For two-dimensional flow, $j = 0$, and for axisymmetric flow, $j = 1$ To complete the foregoing relations, the equation of state

$$p = (R/\bar{M})\rho T \tag{2}$$

where

$$\bar{M} = 1/(\Sigma_i c_i/M_i)$$

is required This equation assumes that the gas consists of a mixture of chemically reacting perfect gases Since the pres sure change across the boundary layer is negligibly small, the equation of state becomes

$$\rho/\rho = \bar{M}T/(\bar{M}\,T) \tag{3}$$

To obtain smoother profiles across the boundary layer which are more readily approximated numerically, and to have the equations in a form compatible with similar solutions, the boundary-layer equations are transformed with the Mangler and Howarth-Dorodnitsyn transformation:

$$\xi(x) = \int_0^x (\rho\mu)\, u\, r_b{}^{2j} dx \qquad \eta(x,y) = \frac{u_e r_b{}^j}{(2\xi)^{1/2}} \int_0^y \rho dy \tag{4a}$$

Then

$$\frac{\partial}{\partial x} = (\rho\mu)\, u\, r_b{}^{2j} \frac{\partial}{\partial \xi} + \frac{\partial \eta}{\partial x} \frac{\partial}{\partial \eta}$$
$$\frac{\partial}{\partial y} = \frac{\rho u_e r_b{}^j}{(2\xi)^{1/2}} \frac{\partial}{\partial \eta} \tag{4b}$$

Also, since we are considering a binary mixture of atoms and molecules the following relations exist:

$$\Sigma_i c_i = c_A + c_M = 1 \tag{5a}$$

$$\Sigma_i \dot{w}_i = \dot{w}_A + \dot{w}_M = 0 \tag{5b}$$

$$Le = Le_{AM} = Le_{MA} \tag{5c}$$

$$Le^T = Le_A{}^T = -Le_M{}^T \tag{5d}$$

$$\bar{c}_p = \Sigma_i c_i c_{p_i} = c_A(c_{p_A} - c_{p_M}) + c_{p_M} \tag{5e}$$

When the foregoing relations (4) and (5) are used with Eqs (1), the boundary-layer equations become

$$2\xi \frac{\partial f'}{\partial \xi} + \frac{\partial V}{\partial \eta} + f' = 0 \tag{6a}$$

$$2\xi f' \frac{\partial f'}{\partial \xi} + V \frac{\partial f'}{\partial \eta} = \beta \left[\frac{\bar{M}}{\bar{M}} \theta - (f')^2 \right] + \frac{\partial}{\partial \eta}\left(l \frac{\partial f'}{\partial \eta} \right) \tag{6b}$$

$$2\xi f' \bar{c}_p \frac{\partial \theta}{\partial \xi} + \bar{c}_p V \frac{\partial \theta}{\partial \eta} = \frac{u^2}{T}\left[l \left(\frac{\partial f'}{\partial \eta} \right)^2 - \beta \frac{\bar{M}_e}{\bar{M}} f'\theta \right] + \frac{\partial}{\partial \eta}\left(\frac{l \bar{c}_p}{Pr} \frac{\partial \theta}{\partial \eta} \right) - \frac{\beta \dot{w}_A (h_A - h_M)}{\rho T\, du/dx} + (c_{p_A} - c_{p_M}) \frac{l}{Pr} \times \left(Le \frac{\partial c_A}{\partial \eta} + \frac{Le^T}{\theta} \frac{\partial \theta}{\partial \eta} \right) \frac{\partial \theta}{\partial \eta} - 2\xi \bar{c}_p \frac{f'\theta}{T} \frac{dT_e}{d\xi} \tag{6c}$$

$$2\xi f' \frac{\partial c_A}{\partial \xi} + V \frac{\partial c_A}{\partial \eta} = \frac{\beta \dot{w}_A}{\rho du_e/dx} + \frac{\partial}{\partial \eta}\left[\frac{l}{Pr} \left(Le \frac{\partial c_A}{\partial \eta} + \frac{Le^T}{\theta} \frac{\partial \theta}{\partial \eta} \right) \right] \tag{6d}$$

where

$$V = \frac{2\xi}{(\rho\mu)_r u\, r_b{}^{2j}} \left(f' \frac{\partial \eta}{\partial x} + \frac{\rho v r_b{}^j}{(2\xi)^{1/2}} \right) \tag{7a}$$

$$\beta = \frac{2\xi}{u} \frac{du_e}{d\xi} \tag{7b}$$

For the boundary conditions, it is assumed that no slip occurs

at the wall, temperature or heat transfer at the body is given, and the wall is catalytic or noncatalytic The boundary conditions for the foregoing boundary-layer equations are as follows:

At the body

$$f'(\xi,0) = 0 \tag{8a}$$

$$V(\xi,0) = (2\xi)^{1/2}(\rho v)_b/[(\rho\mu)\, u\, r_b{}^j] \tag{8b}$$

with specified temperature

$$\theta(\xi,0) = \theta_b(\xi)$$

or specified heat transfer

$$\left.\frac{\partial\theta}{\partial\eta}\right|_b = \left[\frac{[q(2\xi)^{1/2}/\rho u_e r_b{}^j] - (h_M - h_A)(\mu/Pr)Le(\partial c_A/\partial\eta)}{-kT + (h_M - h_A)(\mu/Pr)(Le^T/\theta)}\right]_b \tag{8c}$$

and with catalytic wall

$$c_A(\xi,0) = c_{A\,g}(\theta_b,p) \tag{8d}$$

or with noncatalytic wall

$$\left.\frac{\partial c_A}{\partial\eta}\right|_b = 0 \tag{8e}$$

At the outer edge

$$f'(\xi,\eta) = 1 \qquad \theta(\xi,\eta_e) = 1 \qquad c_A(\xi,\eta) = c_{A_e}(\xi) \tag{9}$$

When there is no injection of fluid at the wall, $V(\xi,0) = 0$ The velocity, temperature, and mass fraction of atoms at the outer edge of the boundary layer are determined from the inviscid flow problem

To obtain the solution of the foregoing boundary-layer equations (6) with boundary conditions (8) an implicit finite-difference scheme is employed as described in the Appendix

B Initial Profiles

As indicated previously, initial profiles are required for the finite-difference solution At the stagnation point or leading edge of a sharp body, as $\xi \to 0$ the continuity equation (6a) becomes

$$(\partial V/\partial\eta) + f' = 0 \tag{10}$$

The mathematical difficulties of the singular point at $\xi = 0$ for a flat plate can be circumvented by having ξ a very small number slightly greater than zero

If we define

$$f = \int_0 f'd\eta \tag{11}$$

then $V = -f$ from Eq (10) With this relation and $\xi \to 0$, the boundary-layer equations (6b–6d) become ordinary differential equations with two-point boundary conditions These equations are solved using the usual iteration techniques employed for similar solutions of the boundary-layer equations

C Exterior Flow

The exterior flow at the edge of the boundary layer is obtained from the inviscid nonequilibrium flow at the surface of the body As the pressure on a body is not affected significantly by the flow being in nonequilibrium and is usually easy to estimate, the pressure distribution is assumed known The ordinary differential equations that govern the flow at the body in terms of the pressure distribution are

$$\frac{du}{dx} = -\frac{1}{\rho u}\frac{dp_e}{dx} \tag{12a}$$

$$\frac{dT_e}{dx} = \frac{1}{\bar{c}_p\rho}\frac{dp_e}{dx} - \dot{w}_A\frac{(h_A - h_M)}{\bar{c}_{p_e}\rho u_e} \tag{12b}$$

$$\frac{dc_{A_e}}{dx} = \frac{\dot{w}_A}{\rho u} \tag{12c}$$

Once the pressure distribution on the body is known, which is preferably obtained from the nonequilibrium flow field solutions, the remaining quantities at the edge of the boundary layer can then be obtained from Eqs (12) Even if the nonequilibrium inviscid flow is known, this procedure is preferred to inputting all the necessary quantities The boundary conditions for Eqs (12), for example, at the stagnation point, are

$$u(0) = 0 \tag{13a}$$

$$T_e(0) = T \tag{13b}$$

$$c_{A_e}(0) = c_A \quad \text{(equilibrium concentration of atoms at temperature } T\text{)} \tag{13c}$$

For other types of bodies these three quantities with the appropriate values are required Since the quantities at the edge of the boundary layer are required as a function of ξ, the differential equation

$$d\xi/dx = (\rho\mu)\, u\, r_b{}^{2j} \tag{14}$$

is solved along with the exterior flow equations (12) to give the desired relation between ξ and x As the exterior flow quantities u, T, and c_A are required at $(m + \frac{1}{2})$ in the transformed plane, and the step-size can change, the following relation for the step size is employed to obtain the results at the desired location:

$$\Delta x_{m+1/2} = \tfrac{1}{2}(\Delta x_{m-1/2} + \Delta x_{m+1/2}) \tag{15}$$

For the first step, $\Delta x_{m-1/2}$ is zero, and $\Delta x_{m+1/2}$ is the desired step size If the step size is changed, the new step size is $\Delta x_{m+1/2}$ The relation

$$\Delta\xi_{m+1/2} = 2(\xi_{m+1/2} - \xi_{m-1/2} - \tfrac{1}{2}\Delta\xi_{m-1/2}) \tag{16}$$

is employed to obtain the step size in the transformed plane

To start the solution of Eq (12) at the stagnation point, certain quantities on the right side of these equations are of an indeterminate form numerically However, it can be shown that, at $x = 0$,

$$\left(\frac{1}{u}\frac{dp}{dx}\right)_s = -\frac{1}{R_N}[2(p - p_\infty)\rho_s]^{1/2} \quad \text{(Newtonian flow)} \tag{17a}$$

$$(\dot{w}_A/u)_s = 0 \tag{17b}$$

For other types of bodies this type of problem does not occur

D Boundary-Layer Characteristics

In addition to the profiles of the various quantities across the boundary layer, parameters that characterize the skin friction, heat transfer, and thickness of the boundary layer are desirable The local skin friction is defined as

$$c_f(Re_x)^{1/2} = \frac{(\rho\mu)_b}{(\rho\mu)}\left(\frac{2u_e x r_b{}^{2j}(\rho\mu)}{\xi}\right)^{1/2}\left(\frac{\partial f'}{\partial\eta}\right)_b \tag{18}$$

The derivative in the foregoing expression is approximated as

$$\left(\frac{\partial f'}{\partial\eta}\right)_b = \left\{\frac{f_2' + (\Delta\eta^2/2l)\beta(\bar{M}_e/\bar{M})\theta}{\Delta\eta[1 + (\Delta\eta/2l)(V - l')]}\right\}_b \tag{19}$$

where no slip at the wall has been assumed At $x = 0$, the following term is of indeterminate form but has the values indicated:

$$[u\, x r_b{}^{2j}(\rho\mu)/\xi]^{1/2} = (2j + 2)^{1/2} \text{ (stagnation point)} \tag{20a}$$

$$[u\, x r_b{}^{2j}(\rho\mu)/\xi]^{1/2} = (2j + 1)^{1/2} \text{ (sharp body)} \tag{20b}$$

The heat-transfer parameter is defined in terms of the Nusselt number and Reynolds number as follows:

$$\frac{Nu}{(Re_x)^{1/2}} = \frac{Pr}{Pr_b}\frac{(\rho\mu)_b}{(\rho\mu)_r}\frac{1}{2^{1/2}}\left(\frac{u_e x r_b^{2j}(\rho\mu)_r}{\xi}\right)^{1/2}\frac{\bar{c}_{p_b}T_e}{(h_{e_s}-h_b)}$$
$$\left\{\frac{\partial\theta}{\partial\eta}+\frac{(h_A-h_M)}{\bar{c}_p T_e}\left(Le\frac{\partial c_A}{\partial\eta}+\frac{Le^T}{\theta}\frac{\partial\theta}{\partial\eta}\right)\right\} \quad (21)$$

where

$$Nu = -q\bar{c}_{p_r}x/[k(h_s-h_b)]$$
$$h = c_A(h_A-h_M)_e + h_{M_{e_s}} + \tfrac{1}{2}u_{e_s}^2$$
$$h_b = c_{A_b}(h_A-h_M)_b + h_{M_b}$$

The derivatives in the expression are approximated as

$$\left.\frac{\partial\theta}{\partial\eta}\right|_b = -\frac{1}{6\Delta\eta}[11\theta_{m\,1}-18\theta_{m\,2}+9\theta_{m\,3}-2\theta_{m\,4}] \quad (22a)$$

$$\left.\frac{\partial c_A}{\partial\eta}\right|_b = -\frac{1}{6\Delta\eta}[11c_{Am\,1}-18c_{Am\,2}+9c_{Am\,3}-2c_{Am\,4}] \quad (22b)$$

The thickness of the boundary layer is depicted by the displacement thickness and in terms of the transformed quantities is

$$\delta^* = \frac{(2\xi)^{1/2}}{\rho u_e r_b^j}\int_0^\eta\left[\left(\frac{1+c_A}{1+c_A}\right)\theta - f'\right]d\eta \quad (23)$$

At the stagnation point, the following term is indeterminate numerically but has the value shown:

$$\frac{(2\xi)^{1/2}}{\rho u_e r_b^j} = \left[-\frac{(\rho\mu)_r u_e}{(j+1)\rho p'}\right]^{1/2} \quad (24)$$

The evaluation of the displacement thickness is obtained with Simpson's method

III Numerical Calculations

A Gas Model

The transport and thermodynamic properties and rate equation are taken to be the same as those employed by Chung and Anderson in order to make a comparison with their results in the first example The binary mixture consists of oxygen atoms and molecules with the following thermodynamic properties:

$$\bar{c}_p = c_{p_A} = c_{p_M} = 7010\ (\text{ft}^2/\text{sec}^2\ °\text{R})$$
$$h_A = c_{p_A}T + 1\,666\times10^8\ (\text{ft}^2/\text{sec}^2)$$
$$h_M = c_{p_M}T$$

The transport properties are such that the following nondimensional parameters are

$$l = 1 \qquad Pr = 1 \text{ or } 0\,7 \qquad Le = 1 \text{ or } 1\,4 \qquad Le^T = 0$$

The rate equation for oxygen,

$$\frac{\dot{w}_A}{\rho} =$$
$$-\frac{(1+c_A)^2(2K_r)\rho^2}{2M_A^2}\left[\frac{c_A^2}{1+c_A}-529\,054\frac{K_p}{p}(1-c_A)\right] \quad (25)$$

where

$$2K_r = 1\,70\times10^{22}/T^2 \qquad K_p = e^{(15\,8-108\,000/T)}$$

was employed in the present examples The foregoing properties are used in the following examples, except the second, where more accurate thermodynamic properties and rate equations are considered One would expect that more accurate transport properties would have a large effect on the boundary-layer characteristics, but this has not been in vestigated

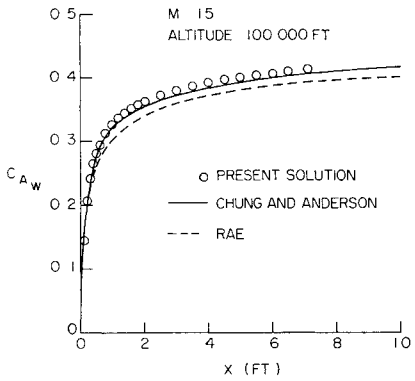

Fig 1 Atom mass fraction at wall for an insulated and noncatalytic flat plate

B Specific Examples

1 *Insulated and noncatalytic flat plate*

The boundary-layer flow on an insulated and noncatalytic flat plate is investigated and compared to result of Chung and Anderson,[3] and Rae [5] For this comparison, the freestream conditions correspond to a Mach number of 15 and an altitude of 100,000 ft (T = 392 4°R and p = 23 4265 psf) The Prandtl and Lewis-Semenov numbers are taken as one in order to have all of the assumptions identical with the other two papers At the outer edge of the boundary layer the oxygen is undissociated and the pressure is taken as a constant throughout the boundary layer

The variation of the atom mass fraction at the wall is given in Fig 1 Also shown in this figure are the results for the same problem as obtained by Chung and Anderson, and Rae Since approximations are required in these two methods, the agreement with the present more exact solution is good

2 *Specified wall temperature and catalytic flat plate*

The flow along a wall with zero pressure gradient T_w/T_e = 3, and zero atom mass fraction at the wall has been investigated In this example, Pr = 0 7 and Le = 1 4 With a freestream velocity of 15 734 fps (Mach number = 15) the boundary layer is essentially "frozen," since the temperature is not high enough for appreciable dissociation to occur The skin friction and heat-transfer parameters are practically constant for the distance considered and are $c_f[Re_x]^{1/2}$ = 0 6645(0 6641) and $Nu/[Re_x]^{1/2}$ = 0 242 (0 248) The values in parentheses are obtained from similar solutions for a perfect gas The displacement thickness of the boundary layer is given in Fig 2 and is approximately the same result as ob tained from similar solution of a perfect gas If the boundary-layer flow is assumed in local equilibrium, the displace ment thickness is slightly less as shown When the freestream velocity is increased to 25,000 fps, there is significant dissociation of oxygen downstream from the leading edge Several temperature and atom mass fraction profiles are pre sented in Figs 3 and 4 In addition to the nonsimilar nonequilibrium profiles (finite-difference solutions), similar pro files for the nonequilibrium flow are presented These solu tions predict a slightly lower temperature while the atom mass fraction is higher The similar solutions are obtained by solving ordinary differential equations with two-point boundary conditions These solutions become exceedingly difficult to obtain downstream from the leading edge as accurate initial guesses of the unknown boundary conditions at the wall are required for the usual integration procedures The local equilibrium profiles, which are the same at all distances along the wall, are significantly different from the nonequilibrium

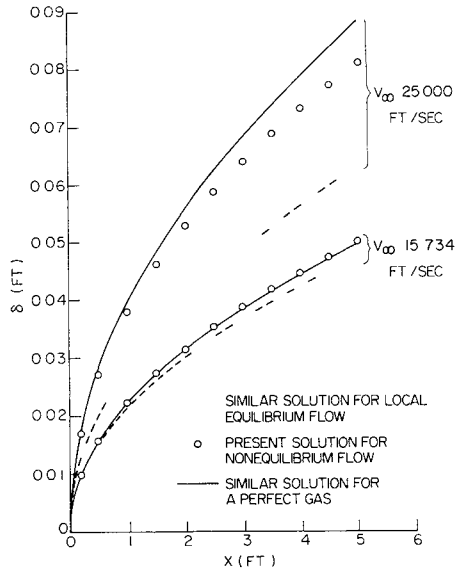

Fig 2 Displacement thickness for flow along a catalytic flat plate with $T_w/T_e = 3$ (alt = 100,000 ft)

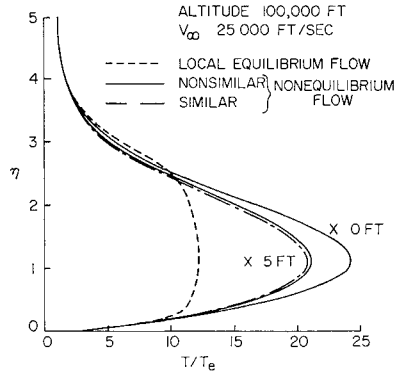

Fig 3 Temperature profiles for a catalytic wall with $T_w/T_e = 3$ and $dp_e/dx = 0$

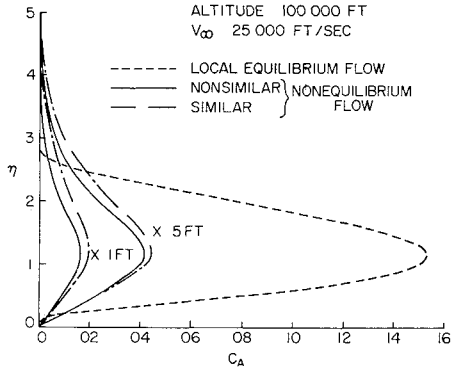

Fig 4 Atom mass fraction profiles for a catalytic wall with $T_w/T_e = 3$ and $dp_e/dx = 0$

profiles, as shown in Figs 3 and 4 The velocity profiles for this example are the Blasius type and remain the same along the wall

The effect on the boundary-layer properties of the rate constants and thermodynamic properties of the gas has been investigated The production of atoms for a binary mixture is written as

$$\frac{\dot{w}_A}{\rho} = \bar{\rho}\frac{c_A}{M_A}\left\{(1-c_A)\left[\left(\frac{1-c_A}{2c_A}\right)k_{f_1}+k_{f_2}\right]-\frac{2\bar{\rho}c_A{}^2}{M_A}\left[\left(\frac{1-c_A}{2c_A}\right)k_{b_1}+k_{b_2}\right]\right\}$$

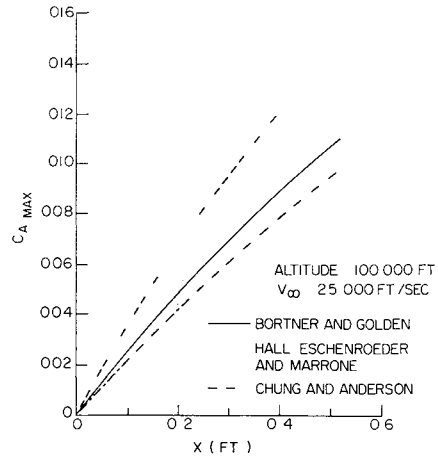

Fig 5 Effect of rate constants on composition of the boundary layer on a catalytic wall with $T_w/T_e = 3$ and $dp_e/dx = 0$

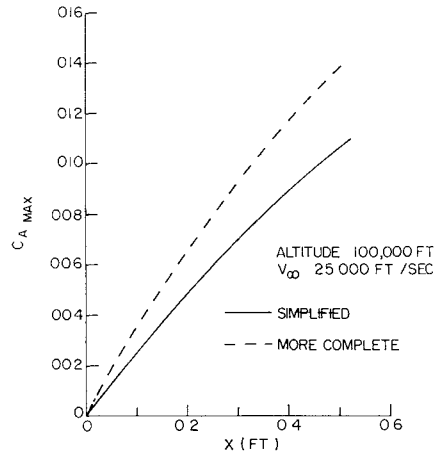

Fig 6 Effect of thermodynamic properties on the composition of the boundary layer on a catalytic wall with $T_w/T_e = 3$ and $dp_e/dx = 0$

where

$$k_f = TK^{C2}\exp(C0 + C1/TK)$$

$$k_b = TK^{D2}\exp(D0 + D1/TK)$$

$$TK = T/1\,8(°\mathrm{K}) \qquad \bar{\rho} = 0\,51536\rho(\mathrm{g/cm^3})$$

The constants used in the foregoing equation and the reference from which they were taken are given in Table 1 The last case gives the same equation as presented previously in (25) The result of using this set of constants is illustrated in Fig 5 where the maximum atom mass fraction in the boundary layer is presented There is a large influence on the composition of the boundary layer by the rate constants employed

The specific heat and enthalpy has been determined from the following expressions which include translational, rotational, and vibrational energies:

$$c_{p_A} = \frac{5}{2}\frac{R}{M_A}$$

$$c_{p_M} = \frac{R}{M_M}\left[\frac{7}{2}+\left(\frac{\theta}{T}\right)^2 e^{\theta/T}(e^{\theta/T}-1)^{-2}\right]$$

$$h_A = \frac{5}{2}\frac{R}{M_A}T + 1\,666\times 10^8$$

$$h_M = \frac{R}{M_M}T\left[\frac{7}{2}+\frac{\theta}{T}(e^{\theta/T}-1)^{-1}\right]$$

where $\theta = 4014°\mathrm{R}$

Table 1 Constants for k_f and k_b

Ref	Reaction	$C0_r$	$C1_r$	$C2_r$	$D0_r$	$D1_r$	$D2_r$
13	$r = 1(O_2 + O_2 \rightleftarrows 2O + O_2)$	40 84869	−59,900	−0 5	37 62982	0	−0 5
	$r = 2(O_2 + O \rightleftarrows 2O + O)$	42 05085	−59,900	−0 5	38 81544	0	−0 5
12	$r = 1(O_2 + O_2 \rightleftarrows 2O + O_2)$	49 63522	−59,380	−1 5	42 54523	0	−1 0
	$r = 2(O_2 + O \rightleftarrows 2O + O)$	42 18847	−59,380	−0 5	35 09847	0	0
3	$r = 1(O_2 + O_2 \rightleftarrows 2O + O_2)$	62 03969	−60,000	−3 0	50 64682	0	−2 0
	$r = 2(O_2 + O \rightleftarrows 2O + O)$	62 03969	−60,000	−3 0	50 64682	0	−2 0

Table 2 Outer edge conditions for 10 cone

Altitude, ft	T_e R	p_e, psf	u_e fps	T_w, R
100 000	1989	630 2	20,600	3600
150,000	2065	72 82	20 600	2160
200,000	2016	11 46	20,590	1620

Table 3 Peak temperature and atom mass fraction for equilibrium

Altitude, ft	$(T_{max}/T_e)_q$	$(\bar{c}_{Am\ x})_q$
100 000	2 71	0 1094
150 000	2 34	0 1032
200 000	2 22	0 1051

With these more complete thermodynamic properties, the same problem has been solved, and the influence on the maximum atom mass fraction is shown in Fig 6

3 Cone with specified wall temperature and catalytic wall

The boundary-layer flow along a 10° cone (half-angle) with zero pressure gradient at three altitudes has been computed The same gas model is employed as discussed earlier in Sec A, and the Prandtl number is 0 7 whereas the Lewis-Somenov number is 1 4 The freestream velocity is taken as 21,000 fps for the three cases considered Since the inviscid flow temperatures are relatively low, the flow at the surface of the cone or the edge of the boundary layer is determined from cone solutions for a perfect gas The boundary conditions at the outer edge of the boundary layer and at the wall for the three cases are shown in Table 2 The oxygen at the edge of the boundary layer and at the wall is considered undissociated because of the low temperatures at these locations

The temperature and atom mass fraction profiles along the cone are presented in Figs 7 and 8 The velocity profiles remain the same along the cone and are the Blasius result At 60 ft from the cone tip, the flow has not reached equilibrium The local equilibrium profiles are shown in these figures and are the same at any distance along the body The maximum temperature and atom mass fraction in the boundary layer are given in Figs 9 and 10 for the three cases The maximum temperature and atom mass fraction as obtained from local equilibrium solutions are given in Table 3 The flow at 200,000 ft is nearly frozen, whereas at 100,000 ft the flow has not reached equilibrium at the distances investigated

The heat transfer by conduction is decreasing along the cone for the nonequilibrium boundary layer as can be seen from Fig 7 The heat transfer by diffusion is increasing along the body which gives a total heat transfer approximately the same for the nonequilibrium and equilibrium boundary layer with a catalytic wall The skin friction is not influenced by the nonequilibrium flow for this case with $l = 1$

4 Hemisphere-cylinder

The nonequilibrium boundary layer has been computed on a hemisphere-cylinder with a 1-ft nose radius The body is considered at an altitude of 225,000 ft with a freestream velocity of 20,000 fps The flow is assumed to be in equilibrium at the stagnation point with the following properties:

$$u = 0 \qquad p = 91\ 322 \text{ psf}$$
$$T = 9880°\text{R} \qquad c_A = 0\ 9993376$$

At this condition the boundary layer is sufficiently thin that the usual interaction with the inviscid flow can be neglected However, the relaxation layer behind the shock wave is becoming large enough that the flow at the edge of the boundary layer could be slightly out of equilibrium

The wall is catalytic with a temperature of 395 2°R; hence, the mass fraction of atoms at the wall is taken at zero To determine the flow at the edge of the boundary layer, the pressure distribution on the body is assumed as shown in Fig 11 The equilibrium pressure distribution shown is a numerical result obtained for the inviscid flow field The flow at the edge of the boundary layer was obtained as discussed in Sec II-C with the assumed pressure In starting the solution at the stagnation point, Eqs (17a) and (17b) were employed with $p_\infty = 0\ 15719$ psf In this example, the density viscosity product at the reference condition is evaluated at the body and is $(\rho\mu) = (\rho\mu)_b (p/p)$

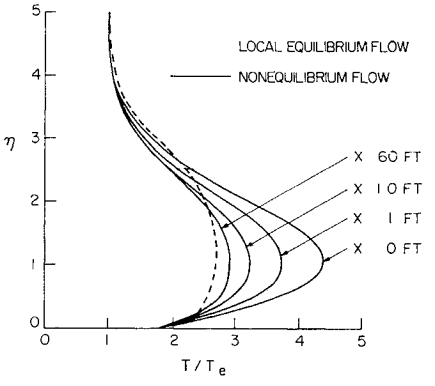

Fig 7 Temperature profiles for a 10 cone at 100,000 ft alt and V_∞ = 21,000 fps

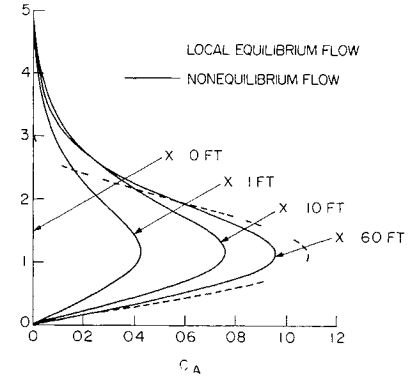

Fig 8 Atom mass fraction profiles for a 10° cone at 100,000 ft alt and V_∞ = 21,000 fps

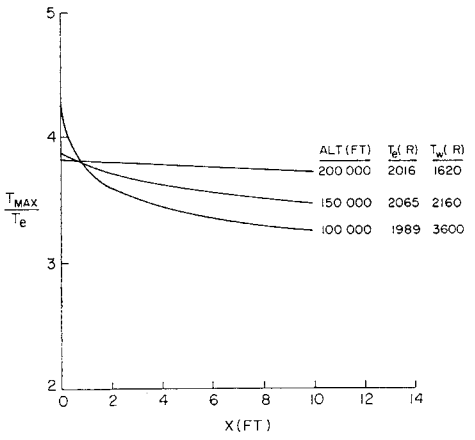

Fig 9 Maximum temperature in boundary layer on a 10° cone (V_∞ = 21,000 fps)

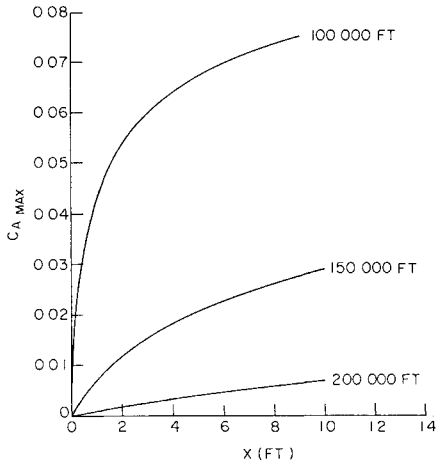

Fig 10 Maximum mass fraction of atoms in boundary layer on 10 cone (V_∞ = 21,000 fps)

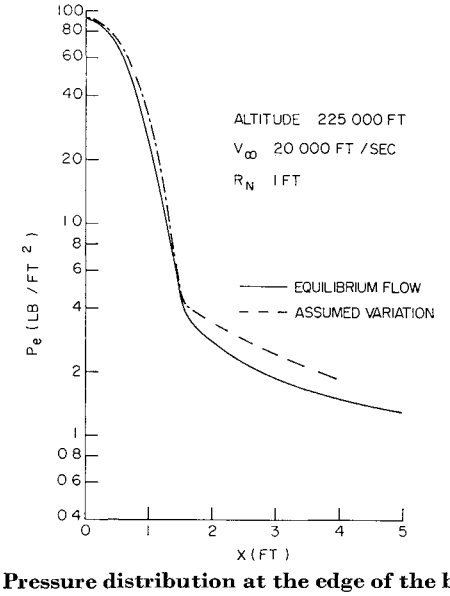

Fig 11 Pressure distribution at the edge of the boundary layer

The computed velocity and temperature at the edge of the boundary layer is given in Fig 12 The flow is frozen since there is no change in the atom mass fraction in the distance investigated For this case, the velocity and temperature on the cylinder at the outer edge of the boundary layer are appreciably smaller than that obtained when the flow is assumed in local equilibrium

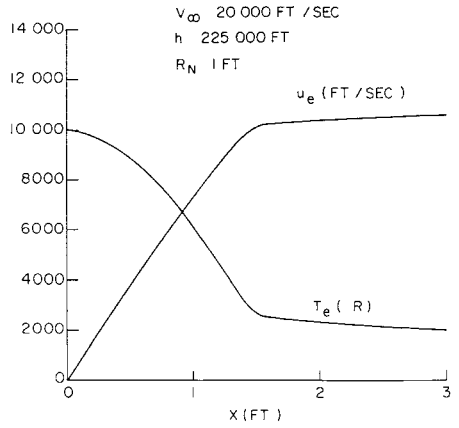

Fig 12 Velocity and temperature at edge of boundary layer for a hemisphere cylinder

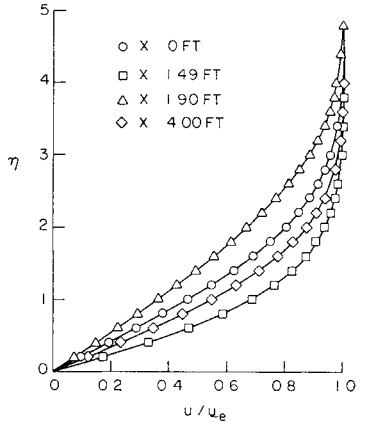

Fig 13 Velocity profiles on the hemisphere cylinder

The boundary layer has been computed from the stagnation point to 4 ft downstream The extreme variation of the velocity profiles are presented in Fig 13 whereas the temperature profiles are given in Fig 14 The atom mass fraction profiles remain nearly the same for the distance computed The heat transfer and skin friction resulting from these profiles are presented in Fig 15 The variation of these parameters is similar to local equilibrium results except for the dip beyond the shoulder for the present case

IV Discussion

The complete partial differential equations of the laminar boundary layer for a chemical nonequilibrium binary gas have been solved with an implicit finite-difference scheme As the equations are solved in a transformed plane where the boundary layer is of nearly uniform thickness, the solution can be started at the stagnation point or leading edge The required initial profiles for starting the solution are similar solutions, which can be readily obtained if not already available As the profiles do not change rapidly in the transformed plane, the solutions are obtained in a reasonable amount of computer time With the implicit procedure employed, there have been no problems of stability or convergence of the solution

With the finite-difference scheme, various boundary conditions have been employed for the nonequilibrium boundary-layer solutions, and results have been obtained on bodies with and without pressure gradients Approximate solutions for a noncatalytic and insulated wall by Chung and Anderson, and Rae are in agreement with the present, more exact results For flows with zero pressure gradient and a catalytic wall, the nonequilibrium effects are unimportant on the heat transfer and skin friction However, the displacement thickness can be greatly changed when there is appreciable dissociation of the gas The results for a cone at 21,000 fps show that the binary flow is nearly frozen at 200,000 ft alt whereas equi

librium has not been obtained at 60 ft from the tip at 100,000 ft The boundary-layer flow on the hemisphere cone at 225,000 ft alt and 20,000 fps is frozen The examples show the importance of considering nonequilibrium flow as the composition and temperature in the boundary layer can be greatly different from local equilibrium or frozen solutions

Nonequilibrium similar solution for a flat plate are reasonably close to the nonsimilar solution However, the time and effort required presently to obtain the similar solutions limits the usefulness, since the nonsimilar results are more accurate and require less time

Extension of the present procedure to a multicomponent fluid is being developed, and in this new program more com plete transport properties will be employed

Appendix: Numerical Solution of the Equations

There are many finite-difference schemes that can be employed to solve the boundary-layer equations In this study an implicit procedure is used that is similar to the method developed in Ref 11 but has been modified so that solutions downstream of stagnation point initial profiles can be obtained The implicit procedures do not have the stability difficulties encountered with explicit schemes, and the truncation error can be of higher order than that of the explict, or Duford-Frankel methods

The flow field is divided into a grid or mesh of size $\Delta\eta$ and $\Delta\xi$ with $x = m\ \Delta\xi$ and $y = n\ \Delta y$ It is assumed that u, θ, and c_A are known at the grid points in the mth column and unknown in the $(m + 1)$th column In the implicit scheme

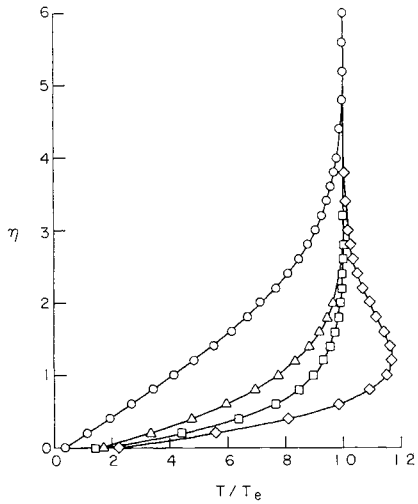

Fig 14 Temperature profiles on the hemisphere cylinder

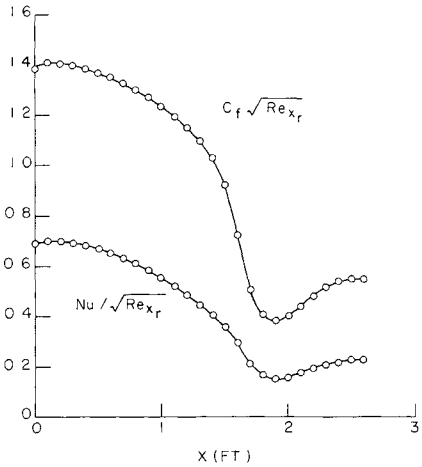

Fig 15 Local skin friction and heat transfer for a hemisphere cylinder

the various types of derivatives must be replaced by linear difference quotients, and the partial differential equations are evaluated at $(m + \frac{1}{2}, n)$ Let functions $H(\xi,\eta)$ and $T(\xi,\eta)$ represent the unknown quantities u, θ, or c_A in the boundary layer, so that the difference quotients at the point $(m + \frac{1}{2}, n)$ are written as

$$\partial H/\partial\xi = (H_{m+1\,n} - H_{m\,n})/\Delta\xi \quad \text{(A1a)}$$

$$\partial H/\partial\eta = \tfrac{1}{2}H_\eta + (H_{m+1\,n+1} - H_{m+1\,n-1})/(4\Delta\eta) \quad \text{(A1b)}$$

$$\partial^2 H/\partial\eta^2 = \tfrac{1}{2}H_{\eta\eta} + (H_{m+1\,n+1} - 2H_{m+1\,n} + H_{m+1\,n-1})/2\Delta\eta^2) \quad \text{(A1c)}$$

$$(\partial H/\partial\eta)^2 = H_\eta(H_{m+1\,n+1} - H_{m+1\,n-1})/(2\Delta\eta) \quad \text{(A1d)}$$

$$(\partial H/\partial\eta)(\partial T/\partial\eta) = [H_\eta(T_{m+1\,n+1} - T_{m+1\,n-1}) + T_\eta(H_{m+1\,n+1} - H_{m+1\,n-1})]/(4\Delta\eta) \quad \text{(A1e)}$$

where

$$H_\eta = (H_{m\,n+1} - H_{m\,n-1})/(2\Delta\eta)$$

$$H_{\eta\eta} = (H_{m\,n+1} - 2H_{m\,n} + H_{m\,n-1})/\Delta\eta^2$$

Product terms are written as

$$H^2 = H_{m\,n}H_{m+1} \quad \text{(A2a)}$$

$$HT = \tfrac{1}{2}(H_{m\,n}T_{m+1\,n} + H_{m+1\,n}T_{m\,n}) \quad \text{(A2b)}$$

In all of the foregoing approximations (A1 and A2), terms of the order $\Delta\xi^2$ and $\Delta\eta^2$ have been neglected To avoid nonlinear difference equations, terms of the following form are approximated as

$$T(\partial H/\partial\xi) = [T_{m\,n} + \tfrac{1}{2}\Delta\xi(\partial T/\partial\xi)_{m\,n} + \quad][(H_{m+1\,n} - H_{m\,n})/\Delta\xi + \quad] \approx T_{m\,n}(H_{m+1\,n} - H_{m\,n})/\Delta\xi \quad \text{(A3)}$$

where terms of the order $\Delta\xi$ have been neglected

When the difference quotients and terms (A1–A3) are substituted in the boundary-layer equations (6), the resulting linear difference equations are written as

$$A_n w_{n+1} + B_n w_n + C_n w_{n-1} = D_n \quad \text{(A4)}$$

where

$$w = \begin{bmatrix} f'_{m+1} \\ \theta_{m+1\,n} \\ c_{Am+1\,n} \end{bmatrix}$$

The matrices A_n, B_n, C_n, and D_n are evaluated at m and the expressions for them are given in Ref 14 Since the simultaneous linear algebraic equations resulting from all of the difference equations (A4) across the boundary layer are of a special form, an efficient algorithm is available (see Ref 15) and is applied to these equations in Ref 14 Thus, the values of w_n are readily computed across the boundary layer

With $f'_{m\,n}$ and $f'_{m+1\,n}$ known, the transformed velocity V is determined from the continuity equation (6a) This equation is evaluated at the point $(n - \frac{1}{2})$ and $(m + \frac{1}{2})$, and the derivatives are written as

$$\partial f'/\partial\xi = (f'_{m+1\,n} + f'_{m+1\,n-1} - f'_{m\,n} - f'_{m\,n-1})/\Delta\xi \quad \text{(A5a)}$$

$$\partial V/\partial\eta = (V_{m+1/2\,n} - V_{m+1/2\,n-1})/\Delta\eta \quad \text{(A5b)}$$

and the quantity $f'_{m+1/2\,n-1/2}$ becomes

$$f'_{m+1/2\,n-1/2} = \tfrac{1}{4}(f'_{m+1\,n} + f'_{m+1\,n-1} + f'_{m\,n} + f'_{m\,n-1}) \quad \text{(A5c)}$$

In the foregoing approximations, quantities of the order of the step size squared are neglected When these relations are substituted into the continuity equation (6a) the unknown transformed velocity becomes

$$V_{n+1/2\,n} = V_{m+1/2\,n-1} - \left(\frac{\xi}{L} + \frac{\Delta\eta}{4}\right)(f'_{m+1\,n} + f'_{m+1\,n-1} + \left(\frac{\xi}{L} - \frac{\Delta\eta}{4}\right)(f'_{m\,n} + f'_{m\,n-1}) \quad \text{(A6)}$$

If iteration is to be performed, the A, B, C, and D matrices are revaluated with the better values of the quantities at $(m + \frac{1}{2}, n)$ now available Then new values of w_n and $V_{m+1/2\,n}$ can be obtained Iteration may be performed at every step or not at all; in either case the foregoing procedure is applied at succeeding steps downstream until the boundary-layer flow along the body is determined

References

[1] Fay, J A and Riddell, F R , "Theory of stagnation point heat transfer in dissociated air," J Aeronaut Sci **25**, 73–85 (1958)

[2] Moore, J A and Pallone, A , "Similar solutions to the laminar boundary-layer equations for nonequilibrium air," Avco Tech Memo RAD TM-62-59 (July 1962)

[3] Chung, P M and Anderson, A D , ' Dissociative relaxation of oxygen over an adiabatic flat plate at hypersonic Mach numbers," NASA TN D-140 (April 1960)

[4] Chung, P M and Anderson, A D , "Heat transfer around blunt bodies with nonequilibrium boundary layers," *Proceedings of the 1960 Heat Transfer and Fluid Mechanics Institute* (Stanford University Press, Stanford, Calif , 1960), pp 150–163

[5] Rae, W J , "An approximate solution for the nonequilibrium boundary layer near the leading edge of a flat plate," IAS Paper 62-178 (June 1962)

[6] Levinsky, E S and Brainerd, J J , "Inviscid and viscous hypersonic nozzle flow with finite rate chemical reactions," Arnold Eng Dev Center TDR-63-18 (January 1963); also IAS Paper 63-63 (1963)

[7] Lees, L , "Laminar heat transfer over blunt nosed bodies at hypersonic flight speeds," Jet Propulsion **26**, 259–269 (1956)

[8] Kemp, N H , Rose, P H , and Detra, R W , "Laminar heat transfer around blunt bodies in dissociated air," J Aerospace Sci **26** (1959)

[9] Moore, F K , "On local flat-plate similarity in the hypersonic boundary layer, J Aerospace Sci **28**, 753–762 (1961)

[10] Blottner, F G , 'Similar and nonsimilar solutions of the nonequilibrium laminar boundary layer, ' AIAA J **1**, 2156–2157 (1963)

[11] Flügge Lotz, I and Blottner, F G , "Computation of the compressible laminar boundary-layer flow including displacement thickness interaction using finite-difference methods, Div Eng Mech , Stanford Univ , TR 131, Air Force Office Sci Res 2206 (January 1962)

[12] Hall, G J , Eschenroeder, A Q , and Marrone, P V , "Inviscid hypersonic airflows with coupled nonequilibrium processes," IAS Paper 62-67 (January 1962); also "Blunt nose inviscid airflows with coupled nonequilibrium processes, ' J Aerospace Sci **29**, 1038–1051 (1962)

[13] Bortner, M H and Golden, J A , "A critique on reaction rate constants involved in the chemical system of high temperature air," General Electric TIS R 61SD023 (February 1961)

[14] Blottner, F G , "Nonequilibrium laminar boundary layer flow of a binary gas,' General Electric TIS R63SD17 (1963); also AIAA Preprint 63 443 (1963)

[15] Richtmyer, R D , *Difference Methods for Initial-Value Problems*, (Interscience Publishers Inc , New York, 1957), pp 101–104

FEBRUARY 1964 AIAA JOURNAL VOL 2, NO 2

Nondimensional Solutions of Flows with Vibrational Relaxation

RALPH PHINNEY*
Martin Marietta Corporation, Baltimore, Md

Vibrational relaxation time data for diatomic gases are reduced to a single curve by a suitable nondimensionalization Using this, together with a previously developed criterion for vibrational freezing, nozzle flow and a simplified blunt-body problem are solved in nondimensional form The effects of freezing on wind tunnel test section and model afterbody conditions are also presented

Nomenclature

A = area
D = nose diameter
E = vibrational energy
J = see Eq (7)
M = Mach no
p = pressure in atmospheres
R = gas constant
r_* = throat radius
T = temperature nondimensionalized with θ
t = time
u = velocity
θ = vibrational characteristic temperature
ρ = density
τ' = relaxation time at atmospheric pressure
τ = relaxation time, τ'/p
ϕ = asymptotic cone half-angle of nozzle
ψ = $(2x/D)$, angle between body tangent and the normal to the freestream velocity

Subscripts

0 = stagnation
* = sonic
∞ = asymptotic, fully expanded flow
e = equilibrium flow
f = frozen flow
F = freeze point value

Received June 13, 1963; revision received October 22, 1963
* Research Scientist, Martin Space Systems Division

Introduction

IN the flow of high-temperature gases, it is commonplace that the relaxation rates associated with various excited states and chemical reactions are not fast enough to permit the gas to remain in equilibrium A number of exact calculations of such flows, combining the flow equations and those for the relaxation, have been made (for example, Refs 1 and 2) These are long and tedious, and, in any case, their accuracy is limited by the usually rather unprecise knowledge of the rate constants Further, it is difficult to draw general conclusions or make parametric studies in this manner

In the expansion process of a nozzle or the flow around a blunt body, the flow of a relaxing gas proceeds from a high-temperature region where the gas is in equilibrium through a transition zone where it departs abruptly from equilibrium This occurs when the temperature and density fall so rapidly that the reaction rate quickly becomes so slow as not to permit continuation of an equilibrium state After the transi